We CO2 10

Experimental And Theoretical Investigation Of Natural Convection In CCS: Onset Time, Mass-Transfer Rate, Capillary Transition Zone, And Heat Of Dissolution

A.A. Eftekhari[1,2]*, R. Farajzadeh[2], H. Bruining[2]
[1]Technical University of Denmark, [2]Delft University of Technology

Summary

We study the enhanced mass transfer of CO2 in water for a CO2 saturated layer on top of a water saturated porous medium, experimentally and theoretically. A relatively large experimental set-up with a length of 0.5 m and a diameter of 0.15 m is used in pressure decay experiments to minimize the error of pressure measurement due to temperature fluctuations and small leakages. The experimental results were compared to the theoretical result in terms of onset time of natural convection and rate of mass transfer of CO2 in the convection dominated process. In addition, a non-isothermal multicomponent flow model in porous media, is solved numerically to study the effect of the heat of dissolution of CO2 in water on the rate of mass transfer of CO2. The effect of the capillary transition zone on the rate of mass transfer of CO2 is also studied theoretically. The simulation results including the effect of the capillary transition zone show a better agreement with experimental results compared to the simulation result without considering a capillary transition zone. The simulation results also show that the effect of heat of dissolution on the rate of mass transfer is negligible

Introduction

Current concern with climate change has increased interest in the usage of low and zero CO_2 emission energy resources. But replacing fossil fuels by sustainable energy resources is a gradual process and cannot be attained in the near future. In the meantime, other measures must be explored and taken to slow down the increasing rate of CO_2 concentration in the atmosphere, which is caused by the combustion of fossil fuels. One of the proposed methods is to separate the CO_2 from flue gas and to store it in geological formations, e.g., injection of supercritical CO_2 into aquifers. The state of the art technology for the separation of CO_2 is amine chemisorption which is effective but very energy intensive. The pipeline transport and injection of supercritical CO_2 requires gas compression, which is among the most energy intensive processes. In average, CO_2 separation from flue gas requires between 2.5 to 4 MJ/kg CO_2 and CO_2 transport via a 150 km pipeline and supercritical aquifer injection requires around 1 MJ/kg CO_2. Coal, with roughly a hydrogen/carbon ratio of one, has 0.088 kg CO_2/MJ while methane with a hydrogen/carbon ratio of four, has 0.055 kg CO2 /MJ, i.e., the largest and smallest carbon dioxide production per unit combustion energy, respectively. Thus a maximum amount of 44% of coal combustion energy and 27% of methane combustion energy are required to achieve the zero emission usage of those fossil fuels, when combined with carbon capture and storage (CCS). Using this high percentage of energy resource cannot be rationalized unless the effectiveness of aquifer storage is demonstrated, i.e., to prove that injected CO_2 will be stored safely underground for a long period of time (Metz, 2005).

Previously the density-driven convection of CO_2 in water, which is one of the methods that can ensure the long-term storage of CO_2, has been studied experimentally and theoretically. The experimental work, which is not as extensive as the theoretical work on this topic, can be subdivided into two main catagories: visualization of fingers by using a Hele-Shaw cell (Faisal et al., 2013; Khosrokhavar et al., 2011; Kneafsey and Pruess, 2010; Mojtaba et al., 2014), and quantification of the dissolution rate in pressure decay or constant pressure experiments in sand packs (Emami-Meybodi et al., 2015; Khosrokhavar et al., 2015; Nazari Moghaddam et al., 2012). The goal of the visualization experiments is to show the instability in the water saturated with CO_2 overlaying a pure water layer and to visualize the formation, initiation, and development of fingers. The major shortcoming of the visualization experiments is the very high permeability of the setup, i.e., several orders of magnitude higher than the permeability of an aquifer. The pressure decay experiments are also conducted in small setup, where the measurements can be easily affected by small leakage. Moreover, the system is usually designed such that only half of the vessel is filled with water saturated sand pack and CO_2 is on the top empty space. This eliminates the important capillary-gravity equilibrium between the two phases and its large effect on the mass transfer rate; see, e.g., (Elenius et al., 2012; Li et al., 2013; Meybodi and Hassanzadeh, 2013).

Here, our objectives of performing the pressure decay experiments are as follows: first, we measure the mass transfer rate of CO_2 in water in a relatively large vessel to reduce the sensitivity of the measurements to small amounts of leakage or temperature fluctuations. These effects are minimized by using a large volume of CO_2 on top of the water saturated porous medium. In addition, by increasing the height of the water layer, we can decrease the permeability of the porous medium to lower (and more realistic) values without changing the Rayleigh number. We also quantify the effect of various rock parameters on the onset time and rate of dissolution and provide experimental data that is missing in the literature. In the theoretical part of this work, we include the effect of heat of dissolution of CO_2 on the rate of mass transfer of CO_2 into water by solving a non-isothermal convection-diffusion equation. We also study the effect of capillary transition zone on the rate of mass transfer.

Experimental method

The experimental set up, shown in Fig., consists of an stainless steel vessel with an inside diameter of 15.24 cm (6 inches) and a height of 62.23 cm (24.5 inches) (see Fig. 1). It is positioned vertically in an oven with a temperature control accuracy of 1 K. The top opening of the vessel is connected to a

pressure transducer with an accuracy of 0.001 bar. The pressure is recorded by data acquisition software every 20 seconds. The experimental procedure is as follows: first, the vessel is completely filled with known mass of sand with a known particle size distribution. To ensure that the sand particles are completely packed, the vessel is shaken by hammering the wall for 30 minutes. The vessel is mounted in the oven and filled with helium at 8 bar. We use the helium detector to check the connections for the leakage. Then we record the helium pressure for 24 hours. If there is no pressure decline (negligible leakage) we flush the sand pack with CO_2 for 10 minutes. Then, we connect the set up to a vacuum pump at -0.9 barg (0.1 bar) for 24 hours. Then a known mass of water is injected through valve 5 to saturate approximately between half to two third of the sand pack. The vacuuming step is necessary to prevent the formation of bubbles of gas in the water saturated zone. Normally, the vacuum in the vessel is enough to suck water inside. In case it cannot transfer the water to the vessel, a piston pump is used to inject the water. The second vessel is filled with CO_2 at 100 bar. We leave the set-up in the oven for 12 hours to reach thermal equilibrium at constant temperature of 35ºC. When the system reached thermal equilibrium, we start the data acquisition system and inject CO_2 into the vessel through valve 3 up to a pressure of around 50 bar. We try to do the injection as slow as possible to minimize the adiabatic expansion effect. The pressure is recorded every 20 seconds for around 5-7 days, depending on the rate of pressure decline.
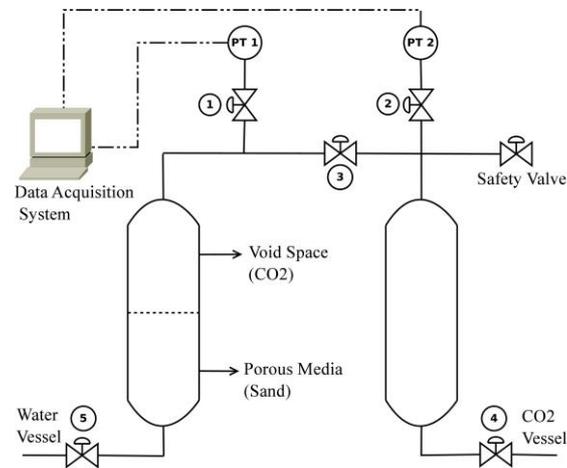

Figure 1 *Schematic representation of the experimental set-up.*

Mathematical model

The saturation of water and gas above the free water (phreatic) level ($p_c = 0$) is considered to be the result of balance between the capillary and gravity forces disregarding the viscous forces due to natural convection flow. The capillary-gravity equilibrium relation reads

$$p_c(S_w) = (\rho_w - \rho_g)gz \qquad (1)$$

where $p_c(S_w)$ [Pa] is the capillary pressure, which is a function of the liquid saturation; ρ_w [kg/m³] and ρ_g [kg/m³] are the densities of the liquid phase and the gas phase, and z [m] is the vertical position relative to the free water (phreatic) level. The capillary pressure data are taken from the number 13 of Plug and Bruining (Plug and Bruining, 2007), which is formulated in terms of

$$p_c(S_w) = \gamma\sigma\sqrt{\frac{\varphi}{k}}\left(\frac{\frac{1}{2} - S_{wc}}{1 - S_{wc}}\right)^{\frac{1}{\lambda_s}}\left(\frac{S_w - S_{wc}}{1 - S_{wc}}\right)^{-\frac{1}{\lambda_s}}. \qquad (2)$$

Here, σ [N/m] is the interfacial tension of CO_2-water, S_{wc} is the connate water saturation, S_w is the liquid saturation, λ_s is the sorting factor, and γ is a constant usually taken equal to 0.5. By substituting p_c from Eq. (2) in Eq. (1), we can calculate the liquid saturation S_w as a function of z, for a log-normal random permeability field with a known Dykstra-Parsons coefficient and correlation length.

The mass balance equation for the non-isothermal flow CO_2-water mixture in porous media (after simplifications) is described by the flowing equations:

$$\varphi \frac{\partial c_{CO_2}}{\partial t} + \nabla .\left(c_{CO_2} \mathbf{u} - \varphi \mathcal{D} \nabla c_{CO_2} \right) = 0, \tag{3}$$

$$\nabla .\left(\frac{k}{\mu} \nabla p \right) = \nabla .\left[\frac{k}{\mu} \left(\left[(\beta_c - 1) M_{water} + M_{CO_2} \right] c_{CO_2} + \frac{M_{water}}{v_{water}} \right) \mathbf{g} \right], \tag{4}$$

$$\alpha \frac{\partial T}{\partial t} + \nabla .\left[-\left(\sum_i \hat{c}_{p,i} \varphi \mathcal{D}_i \nabla c_i \right) T \right] + \nabla .[-\lambda \nabla T] + \nabla .\left[\left(\mathbf{u} \sum_i c_i \hat{c}_{p,i} \right) T \right] + S = 0, \tag{5}$$

$$\alpha = \varphi \left(c_{CO_2} \hat{c}_{p,CO_2} + c_{water} \hat{c}_{p,water} \right) + (1-\varphi) \rho^s c_p^s, \tag{6}$$

$$S = \nabla .\left[-\sum_i \hat{h}_{0,i} \varphi \mathcal{D}_i \nabla c_i \right] + \nabla .\left[\mathbf{u} \sum_i c_i \hat{h}_{0,i} \right]. \tag{7}$$

where c_{CO2} [mol/m^3] is the molar concentration of CO_2 , M_{water} and M_{CO2} [kg/mol] are the molecular weight of water and CO_2 , v_{water} [m^3/mol] is the molar volume of pure water and β_c is a dimensionless coefficient, which is a function of pressure and temperature but composition independent, c_p^s [J/(kg.K)] is the heat capacity of the porous medium, h_0^s [J/kg] is the enthalpy of the solid phase at the reference temperature, $\hat{h}_i$ [J/mol] is the partial molar enthalpy of component i, and $\hat{c}_{p,i}$ [J/(mol.K)] and $\hat{h}_{0,i}$ [J/mol] are constants for the calculation of partial molar enthalpy of component i. We solve the above equations for four different scenarios, viz., a sharp horizontal interface between the water and CO_2 (isothermal and nonisothermal), a capillary transition zone between water and CO_2 represented by unmovable blobs of water, and a capillary transition zone as a region with high diffusivity of CO_2 in water, and a lower permeability as proposed by Elenius et al. (Elenius et al., 2012). For more details of the model, and its boundary conditions, see (Eftekhari, 2013).
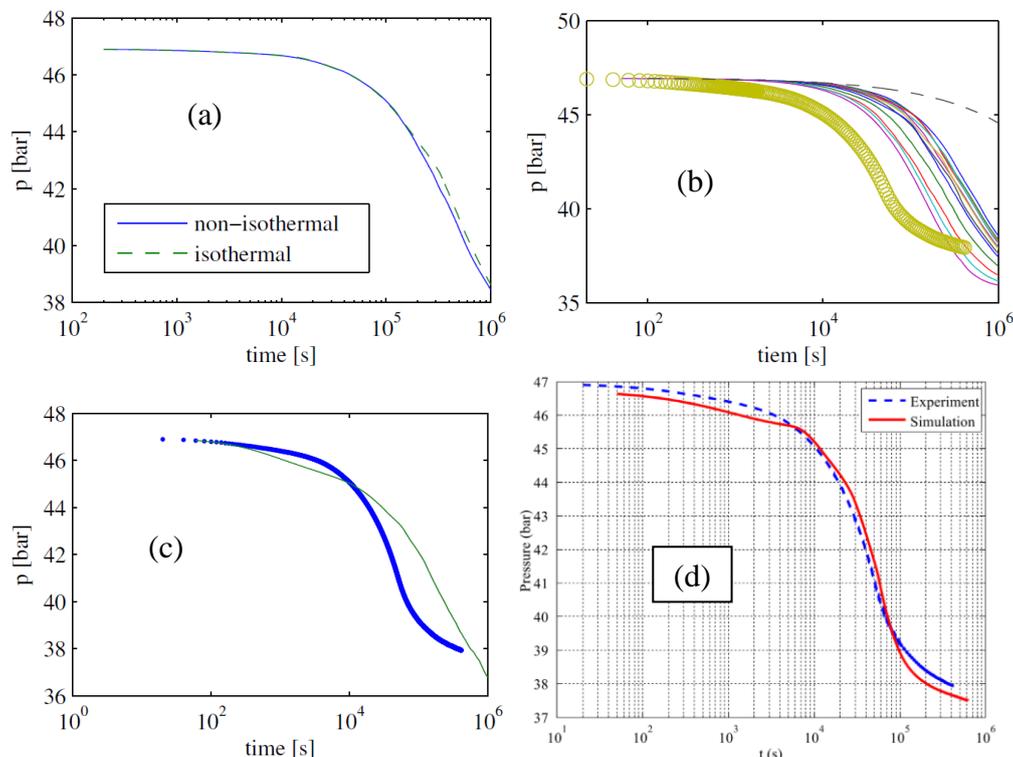
Results and discussion

Figure 2 *(a) a comparison betwee the isothermal and non-isothermal simulations; (b) Simulation results compared with the experimental data (circular marker) and diffusion model (dashed line), for different permeability values; simulation results vs experimental data for a capillary transition zone with (c) unmovable blobs of water, and (d) a region with high CO_2 diffusivity.*

The simulation results are compared with the experimental data in Fig. 2-(a) to (d). The heat of dissolution of the CO_2 in water does not have any significant effect on the rate of mass transfer (Fig. 2-a). Fig. 2-b depicts the results without considering a capillary transition zone, which shows that the model is not able to fit the experimental data without considering a capillary transition zone. Figs. 2-c and 2-d show that the onset of convection is better predicted by including a capillary transition zone in the model; the model that represents the capillary transition zone with a high CO_2 diffusivity gives the best fit to the experimental data.

Conclusions

We performed a set of pressure decay experiments in a relatively large experimental set-up to measure the onset time of natural convection and the rate of mass transfer of CO_2 into water-saturated porous media. We used a mathematical model to study the effect of heat of dissolution of CO_2 on the rate of mass transfer. The effect of heat of dissolution of CO_2 in water on the rate of mass transfer is negligible. We compared various relations for the calculation of onset time with the deviation of experimentally measured pressure decay data from calculated pressure decay data for a pure diffusion model. We studied the effect of a capillary transition zone on the density-driven flow of CO_2 in water. A capillary transition zone can considerably increase the mass transfer rate of CO_2 in water. Our numerical simulations give the best match with experimental pressure decay data when a capillary transition zone is considered in the mathematical model.

References
Eftekhari, A.A., [2013]. Low Emission Conversion of Fossil Fuels with Simultaneous or Consecutive Storage of Carbon Dioxide. PhD thesis, Delft University of Technology.
Elenius, M.T., Nordbotten, J.M., Kalisch, H., [2012]. Effects of a capillary transition zone on the stability of a diffusive boundary layer. IMA J. Appl. Math. 77, 771–787.
Emami-Meybodi, H., Hassanzadeh, H., Green, C.P., Ennis-King, J., [2015]. Convective dissolution of CO2 in saline aquifers: Progress in modeling and experiments. Int. J. Greenh. Gas Control 40, 238–266.
Faisal, T.F., Chevalier, S., Sassi, M., [2013]. Experimental and numerical studies of density driven natural convection in saturated porous media with application to CO2 geological storage. Energy Procedia 37, 5323–5330.
Khosrokhavar, R., Eftekhari, A.A., Farajzadeh, R., Bruining, J., [2015]. Effect of Salinity and Pressure on the Rate of Mass Transfer in Aquifer Storage of Carbon Dioxide, in: 18th European Symposium on Improved Oil Recovery – Dresden.
Khosrokhavar, R., Elsinga, G., Mojaddam, A., Farajzadeh, R., Bruining, J., [2011]. Visualization of Natural Convection Flow of (Sub-) and (Super-) Critical CO_2 in Aqueous and Oleic Systems by Applying Schlieren Method, in: SPE EUROPEC/EAGE Annual Conference and Exhibition. Society of Petroleum Engineers, Vienna, Austria. doi:10.2118/143264-MS
Kneafsey, T.J., Pruess, K., [2010]. Laboratory flow experiments for visualizing carbon dioxide-induced, density-driven brine convection. Transp. Porous Media 82, 123–139.
Li, B., Tchelepi, H.A., Benson, S.M., [2013]. Influence of capillary-pressure models on CO 2 solubility trapping. Adv. Water Resour. 62, 488–498.
Metz, B., [2005]. Carbon Dioxide Capture and Storage: Special Report of the Intergovernmental Panel on Climate Change. Cambridge University Press.
Meybodi, H.E., Hassanzadeh, H., [2013]. Stability analysis of two-phase buoyancy-driven flow in the presence of a capillary transition zone. Phys. Rev. E 87, 033009.
Mojtaba, S., Behzad, R., Rasoul, N.M., Mohammad, R., [2014]. Experimental study of density-driven convection effects on CO2 dissolution rate in formation water for geological storage. J. Nat. Gas Sci. Eng. 21, 600–607.
Nazari Moghaddam, R., Rostami, B., Pourafshary, P., Fallahzadeh, Y., [2012]. Quantification of density-driven natural convection for dissolution mechanism in CO_2 sequestration. Transp. Porous Media 92, 439–456.
Plug, W.-J., Bruining, J., [2007]. Capillary pressure for the sand–CO2–water system under various pressure conditions. Application to CO2 sequestration. Adv. Water Resour. 30, 2339–2353.